J. Fluid Mech. (1999), *vol.* 379, *pp.* 1–22. Printed in the United Kingdom

Similarity in non-rotating and rotating turbulent pipe flows

By MARTIN OBERLACK†

Center for Turbulence Research, Stanford University, CA 94305-3030, USA

(Received 5 March 1997 and in revised form 12 February 1998)

The Lie group approach developed by Oberlack (1997) is used to derive new scaling laws for high-Reynolds-number turbulent pipe flows. The scaling laws, or, in the methodology of Lie groups, the invariant solutions, are based on the mean and fluctuation momentum equations. For their derivation no assumptions other than similarity of the Navier–Stokes equations have been introduced where the Reynolds decomposition into the mean and fluctuation quantities has been implemented. The set of solutions for the axial mean velocity includes a logarithmic scaling law, which is distinct from the usual law of the wall, and an algebraic scaling law. Furthermore, an algebraic scaling law for the azimuthal mean velocity is obtained. In all scaling laws the origin of the independent coordinate is located on the pipe axis, which is in contrast to the usual wall-based scaling laws. The present scaling laws show good agreement with both experimental and DNS data. As observed in experiments, it is shown that the axial mean velocity normalized with the mean bulk velocity $\bar{u}_m$ has a fixed point where the mean velocity equals the bulk velocity independent of the Reynolds number. An approximate location for the fixed point on the pipe radius is also given. All invariant solutions are consistent with all higher-order correlation equations. A large-Reynolds-number asymptotic expansion of the Navier–Stokes equations on the curved wall has been utilized to show that the near-wall scaling laws for flat surfaces also apply to the near-wall regions of the turbulent pipe flow.

1. Introduction

Many researchers have investigated turbulent pipe flows in detail over the last hundred years, including flows with Reynolds numbers of up to $Re_m = 3.5 \times 10^7$ (for references see Zagarola 1996). However, little agreement has been accomplished concerning the analytic form of the mean profile in the centre of the flow. Almost all proposed functional forms of the mean flow may be written in the usual defect-law scaling

$$\frac{\bar{u}_c - \bar{u}}{u_\tau} = f\left(\frac{y}{R}\right), \tag{1.1}$$

first introduced by Stanton & Pannel (1914), where $\bar{u}$, $\bar{u}_c$, u_τ, R and y are, respectively, the mean velocity, the centreline velocity, the friction velocity, the pipe radius and the distance from the wall. Based on empirical arguments, different functions have been proposed for f (see Schlichting 1979). One of the earliest attempts to describe the

† Permanent address: Institut für Technische Mechanik, RWTH Aachen, Templergraben 64, 52056 Aachen, Germany.

mean flow in the centre of a turbulent pipe flow was made by Darcy (1858):

$$\frac{\bar{u}_c - \bar{u}}{u_\tau} = 5.08 \left(1 - \frac{y}{R}\right)^{3/2}. \tag{1.2}$$

It will be shown later that Darcy's law is consistent with the results of the present investigation. Von Kármán (1930) developed one of the many different scaling laws for the mean flow in a pipe based on the mixing-length model introduced by Prandtl (1925).

A related flow problem which exhibits additional interesting flow features is that of the turbulent flow in a pipe rotating about its axis. One of the earliest experimental investigations on this problem was conducted by Levy (1929). He found that the friction coefficient is reduced as the rotation rate was increased. The first detailed measurements of the mean velocity profiles were made by Murakami & Kikuyama (1980) and Kikuyama *et al.* (1983). They reported significant changes in the turbulent characteristics of the rotating pipe flow, including relaminarization. The azimuthal velocity fitted an algebraic scaling law with an exponent of approximately 2. Almost no dependence of the exponent on the axial and azimuthal Reynolds number was found when the velocity was normalized with the wall friction velocity. This has been confirmed in recent measurements by Reich (1988). The algebraic azimuthal mean velocity profile is in sharp contrast to the laminar flow in a rotating pipe, where solid-body rotation occurs (Kikuyama *et al.* 1983; Reich 1988). Recently DNS calculations of a rotating pipe flow by Orlandi & Fatica (1997) and DNS and LES calculations by Eggels, Boersma & Nieuwstadt (1996) have been reported. The calculations support the findings of the experiments. Orlandi & Fatica (1997) did detailed investigations on coherent structures. In the rotating pipe flow, elongated streamwise structures near the pipe axis are found.

To mathematically describe the rotating pipe flow, modelling approaches have been introduced. The most simple approaches have been based on the mixing-length model introduced by Kikuyama *et al.* (1983) and Reich (1988). However, in both investigations the algebraic scaling law for the azimuthal velocity was an input to the model and not a result. Only the deformation of the axial mean velocity due to the rotation was calculated. Hirai, Takagi & Matsumoto (1988) have tested three different models for the problem of a rotating pipe flow: (i) the classical k–ε model by Jones & Launder (1973), (ii) a modified k–ε model which accounts for Richardson number effects by Launder, Priddin & Sharma (1977) and (iii) the second-moment closure model of Launder, Reece & Rodi (1975). The results from the standard k–ε model were unaffected by the rotation. The modified k–ε model accounted for system rotation but was not able to capture any of the correct physical trends for the mean flow found in experiments. Only the second-moment closure model could qualitatively describe both mean flow profiles.

Another phenomenon of a high-Reynolds-number turbulent pipe flow, first reported by Preston (1950), is a fixed point in the mean axial velocity normalized with the bulk velocity. The point is independent of Reynolds number and all mean velocity profiles collapse at $r/R = 0.75$, where r is the radial coordinate. A detailed experimental verification of this mean flow behaviour over a wide range of Reynolds numbers has been conducted by Zagarola *et al.* (1996). A phenomenon similar to the fixed point in a non-rotating pipe flow has been observed in a rotating pipe flow by Reich (1988) when the rotation rate is varied. An explanation for both phenomena will be given employing the new scaling law derived herein.

To give a mathematical theory of the observed phenomena of a non-rotating and

a rotating pipe flow based on first principles rather than on modelling, the approach developed by Oberlack (1997) will be adopted. Therein, a method was developed to obtain scaling laws in plane parallel turbulent shear flows from the Navier–Stokes equations where the Reynolds decomposition into mean and fluctuating quantities has been employed. The approach is based on the classical Lie group analysis to ensure that all self-similar, or, in the methodology of Lie groups, all invariant solutions, are obtained. The results therein cover the usual law of the wall as well as introducing several new scaling laws. These include an algebraic and an exponential scaling law. All of the scaling laws were verified using both experimental and DNS data. In the following it will be shown that the application of the Lie group approach to cylindrical turbulent flows provides explanations for many of the pipe flow phenomena described above and new pipe flow scaling laws will be derived.

A first attempt using Lie group methods in turbulence has been undertaken by Ünal (1994) and Ibragimov & Ünal (1994) analysing Kolmogorov's inertial-subrange theory. Therein it is demonstrated by investigating the symmetries of the Navier–Stokes equations that the dissipation rate may be an invariant if a certain linear combination of two scaling symmetries is chosen.

Lie group analysis, also called symmetry analysis, was developed by Sophius Lie to find point transformations which map a given differential equation to itself. Lie realized that his method unifies almost all known exact integration techniques for both ordinary and partial differential equations. Furthermore, it can be applied to arbitrary nonlinear equations where no general integration methods are known. Group analysis is the only rigorous mathematical method to find all symmetries of a given differential equation and no *ad hoc* assumptions or *a priori* knowledge of the equation under investigation is needed. Once the symmetries are known they can be utilized in a variety of applications. The most useful application for ordinary differential equations is the reduction of order or, depending on the structure of the symmetries, the complete integration of the equation. The most widespread application for partial differential equations is the derivation of self-similar solutions, also called symmetry reduction. Another usage is the derivation of new solutions from old ones. With group analysis it can also be examined whether a nonlinear differential equation is linearizable or whether a linear differential equation can be transformed to a linear constant-coefficient equation.

If group methods are applied to the Navier–Stokes equations (where no averaging has been inferred) one obtains all the axiomatic transformation properties of classical mechanics such as scaling invariance, frame invariance with respect to finite rotation, frame invariance with respect to translation in space and time, Galilean invariance and its generalization and two-dimensional material frame indifference. Almost all known exact solutions of the Navier–Stokes equations emerge from the latter symmetries.

Classical approaches such as dimensional analysis or *ad hoc* methods usually capture only a few symmetries and normally strongly depend on intuition. Furthermore, it may be difficult to prove with the classical methods whether all self-similar solutions have been found, but this is guaranteed with Lie group analysis. The theory is fully algorithmic and no *a priori* knowledge of the equation is needed. Modern approaches to group theory applied to differential equations are presented in Hill (1992) or more for a more thorough discussion of the topic in Bluman & Kumei (1989), Ibragimov (1994, 1995) and Olver (1986).

Scaling laws are not isolated features of certain turbulent flows but mirror the symmetries of the Navier–Stokes equations. To understand the mechanisms and the underlying physics of turbulence, symmetries are very important features in particular

in view of improved turbulence models. Many of the common turbulence models, and in particular the most widespread k–ε model, violate symmetry properties of the Navier–Stokes equations. The model study of the rotating pipe flow problem as accomplished by Hirai *et al.* (1988) illuminates the inability of the k–ε model to properly emulate turbulent flows with strong streamline curvature. In the rotating pipe problem the k–ε model yields solid-body rotation which is not supported by experimental and DNS data.

The paper is organized as follows. In § 2 the governing equations are derived and a brief introduction to the theory developed in Oberlack (1997) is given. In § 3 the Lie group analysis of circular turbulent flows is presented and self-similar mean velocity profiles are calculated. In § 4 the self-similar solutions are compared with experimental and DNS data. In §§ 3 and 4 only outer flow scaling laws are derived and the classical near-wall scaling laws are not captured. Hence, in § 5 a regular asymptotic expansion of the Navier–Stokes equations on the curved wall will be utilized to show that near-wall scaling laws can be obtained from flat-surface scaling laws in the limit of large Reynolds numbers. Section 6 deals with the fixed point of the mean axial velocity normalized with the bulk velocity in a non-rotating and rotating pipe.

All the present results have been aided by SYMMGRP.MAX, a Lie group software package for MACSYMA (1993) written by Champagne, Hereman & Winternitz (1991).

2. Governing equations

The basis for the following analysis is the incompressible Navier–Stokes equations in cylinder coordinates at a constantly rotating frame of reference about the z-axis:

$$\frac{\partial U_z}{\partial t} + U_z\frac{\partial U_z}{\partial z} + U_r\frac{\partial U_z}{\partial r} + \frac{U_\phi}{r}\frac{\partial U_z}{\partial \phi} = -\frac{\partial P}{\partial z} + \nu\left[\frac{\partial^2 U_z}{\partial z^2} + \frac{1}{r}\frac{\partial}{\partial r}\left(r\frac{\partial U_z}{\partial r}\right) + \frac{1}{r^2}\frac{\partial^2 U_z}{\partial \phi^2}\right], \tag{2.1a}$$

$$\frac{\partial U_r}{\partial t} + U_z\frac{\partial U_r}{\partial z} + U_r\frac{\partial U_r}{\partial r} + \frac{U_\phi}{r}\frac{\partial U_r}{\partial \phi} - \frac{U_\phi^2}{r} = -\frac{\partial P}{\partial r} + \nu\left[\frac{\partial^2 U_r}{\partial z^2} + \frac{\partial}{\partial r}\left(\frac{1}{r}\frac{\partial}{\partial r}(rU_r)\right) + \frac{1}{r^2}\frac{\partial^2 U_r}{\partial \phi^2} - \frac{2}{r^2}\frac{\partial U_\phi}{\partial \phi}\right] + 2\Omega U_\phi, \tag{2.1b}$$

$$\frac{\partial U_\phi}{\partial t} + U_z\frac{\partial U_\phi}{\partial z} + U_r\frac{\partial U_\phi}{\partial r} + \frac{U_\phi}{r}\frac{\partial U_\phi}{\partial \phi} + \frac{U_\phi U_r}{r} = -\frac{1}{r}\frac{\partial P}{\partial \phi} + \nu\left[\frac{\partial^2 U_\phi}{\partial z^2} + \frac{\partial}{\partial r}\left(\frac{1}{r}\frac{\partial}{\partial r}(rU_\phi)\right) + \frac{1}{r^2}\frac{\partial^2 U_\phi}{\partial \phi^2} + \frac{2}{r^2}\frac{\partial U_r}{\partial \phi}\right] - 2\Omega U_r \tag{2.1c}$$

and the continuity equation

$$\frac{\partial U_z}{\partial z} + \frac{1}{r}\frac{\partial}{\partial r}(rU_r) + \frac{1}{r}\frac{\partial U_\phi}{\partial \phi} = 0, \tag{2.2}$$

where U_z, U_r, U_ϕ, P, ν and $\Omega_z = \Omega$, are, respectively, the instantaneous velocity vector in the axial, radial and azimuthal directions, the pressure, the kinematic viscosity, and the angular rotation rate of the frame of reference. In equation (2.1), and subsequently, the pressure has been normalized with the density.

Due to the rotational symmetry in a fully developed straight pipe flow, all mean quantities depend only on the radial coordinate r. The only mean velocities that need to be considered are in the axial and the azimuthal directions. The standard Reynolds decomposition for the pressure and the velocities in cylinder coordinates is $P = \bar{p} + p$, $U_z = \bar{u}_z + u_z$, $U_\phi = \bar{u}_\phi + u_\phi$, and $U_r = \bar{u}_r + u_r$, where the overbar denotes an ensemble average and the lower-case letters refer to the fluctuating quantities.

The mean pressure consists of an axial part coming from a constant pressure gradient along the pipe axis and a radial part due to the turbulent normal stresses. Hence, in the following $\bar{p}$ will be replaced with $-Kz + \bar{p}$ where $\bar{p}$ depends only on r and K refers to the constant pressure gradient. In case of a rotating pipe flow the normal stresses also contain centrifugal forces.

The present analysis is restricted to stationary parallel mean shear flows. Hence the equations

$$\frac{\partial \bar{u}_z}{\partial z} = \frac{\partial \bar{u}_z}{\partial \phi} = \frac{\partial \bar{u}_z}{\partial t} = \frac{\partial \bar{u}_\phi}{\partial z} = \frac{\partial \bar{u}_\phi}{\partial \phi} = \frac{\partial \bar{u}_\phi}{\partial t} = \frac{\partial \bar{p}}{\partial z} = \frac{\partial \bar{p}}{\partial \phi} = \frac{\partial \bar{p}}{\partial t} = \bar{u}_r = 0 \tag{2.3}$$

need to be employed in the subsequent analysis.

In the present investigation only the mean velocities are analysed and hence there is no need to derive a separate equation for the mean and the fluctuation quantities. Mean convective terms are not present in the flow and for parallel flows there is a one-to-one relationship between the Reynolds stresses, the pressure gradient, and the viscous stresses. The Reynolds decomposition can be directly used in the equations (2.1) and (2.2) to obtain the somewhat unusual form of the Navier–Stokes equations in cylindrical coordinates:

$$\mathscr{N}_1 = \frac{\partial u_z}{\partial t} + (\bar{u}_z + u_z)\frac{\partial u_z}{\partial z} + u_r \frac{\partial (\bar{u}_z + u_z)}{\partial r} + \frac{\bar{u}_\phi + u_\phi}{r}\frac{\partial u_z}{\partial \phi} + \frac{\partial p}{\partial z} - K - \nu\left[\frac{\partial^2 u_z}{\partial z^2} + \frac{1}{r}\frac{\partial}{\partial r}\left(r\frac{\partial (\bar{u}_z + u_z)}{\partial r}\right) + \frac{1}{r^2}\frac{\partial^2 u_z}{\partial \phi^2}\right] = 0, \tag{2.4a}$$

$$\mathscr{N}_2 = \frac{\partial u_r}{\partial t} + (\bar{u}_z + u_z)\frac{\partial u_r}{\partial z} + u_r \frac{\partial u_r}{\partial r} + \frac{\bar{u}_\phi + u_\phi}{r}\frac{\partial u_r}{\partial \phi} - \frac{(\bar{u}_\phi + u_\phi)^2}{r} + \frac{\partial \bar{p}}{\partial r} + \frac{\partial p}{\partial r} - \nu\left[\frac{\partial^2 u_r}{\partial z^2} + \frac{\partial}{\partial r}\left(\frac{1}{r}\frac{\partial}{\partial r}(r u_r)\right) + \frac{1}{r^2}\frac{\partial^2 u_r}{\partial \phi^2} - \frac{2}{r^2}\frac{\partial u_\phi}{\partial \phi}\right] - 2\Omega(\bar{u}_\phi + u_\phi) = 0, \tag{2.4b}$$

$$\mathscr{N}_3 = \frac{\partial u_\phi}{\partial t} + (\bar{u}_z + u_z)\frac{\partial u_\phi}{\partial z} + u_r \frac{\partial (\bar{u}_\phi + u_\phi)}{\partial r} + \frac{\bar{u}_\phi + u_\phi}{r}\frac{\partial u_\phi}{\partial \phi} + \frac{(\bar{u}_\phi + u_\phi)u_r}{r} + \frac{1}{r}\frac{\partial p}{\partial \phi} - \nu\left[\frac{\partial^2 u_\phi}{\partial z^2} + \frac{\partial}{\partial r}\left(\frac{1}{r}\frac{\partial}{\partial r}(r(\bar{u}_\phi + u_\phi))\right) + \frac{1}{r^2}\frac{\partial^2 u_\phi}{\partial \phi^2} + \frac{2}{r^2}\frac{\partial u_r}{\partial \phi}\right] + 2\Omega u_r = 0. \tag{2.4c}$$

The above equations are written in the form $\mathscr{N}_i = 0$ for later convenience in the Lie group analysis.

The continuity equation (2.2) stays unchanged with the instantaneous velocities interchanged with the fluctuation velocities,

$$\mathscr{C} = \frac{\partial u_z}{\partial z} + \frac{1}{r}\frac{\partial}{\partial r}(r u_r) + \frac{1}{r}\frac{\partial u_\phi}{\partial \phi} = 0. \tag{2.5}$$

The system (2.4) and (2.5) forms a set of unclosed equations in the sense that it contains more dependent variables than equations. This usually requires the introduc-

tion of higher-order statistical moment equations to find turbulent scaling laws. In the present investigation this is not necessary. In Oberlack (1997) it was shown that in order to obtain turbulent scaling laws for the mean flow, only the equations for the mean velocity and the second-order velocity product equations (VPE) have to be considered. In the following the VPE will refer to the usual second-moment equations, where the averaging process has been omitted. As a consequence, all scaling laws are consistent with the Reynolds-stress transport equations. The converse may not be true, since the averaging process is not reversible. In appendix B in Oberlack (1997) it was shown that the self-similar mean velocities derived from the VPE approach are also obtainable by analysing the two-point correlation equations in physical space.

Since the cylindrical coordinate system is orthogonal, the VPE may be written as the dyadic product

$$\mathscr{N}_i u_j + \mathscr{N}_j u_i = 0, \tag{2.6}$$

where $u_1 = u_z$, $u_2 = u_r$, and $u_3 = u_\phi$.

The present investigation has two advantages over an analysis that considers the mean momentum and the Reynolds stress equations. First, in the usual second-moment equations a large number of unclosed terms need to be considered. In principle all infinite higher-order correlations need to be considered to show that the scaling laws obtained below are consistent with all higher-order-correlation equations. Lie group analysis with today's computer algebra systems can only be applied to finite and fairly small systems. Secondly, in appendix A of Oberlack (1997) it was proven that no higher than the second-order-moment equations (2.6) were needed to have the resulting mean velocity scaling laws consistent with all higher-order-moment equations. It will be shown later that this also applies to the present investigation.

3. Symmetry analysis for the turbulent pipe flow

In the following, the Lie group approach developed in Oberlack (1997) will be applied to non-rotating and rotating pipe flow to obtain all self-similar or also called invariant solutions. In the present case the analysis includes the variables

$$\boldsymbol{y} = \{z,\ r,\ \phi,\ t,\ v,\ u_z,\ u_r,\ u_\phi,\ p,\ \bar{u}_z,\ \bar{u}_\phi,\ \bar{p}\}. \tag{3.1}$$

Note that (3.1) contains v as an additional variable. This is a classical idea in Lie group analysis (see e.g. Bluman & Kumei 1989) and is called equivalence transformation. It was first applied to Navier–Stokes equations in its usual form in Ünal (1994).

The purpose of the symmetry analysis is to find those transformations

$$\boldsymbol{y}^* = \{z^*,\ r^*,\ \phi^*,\ t^*,\ v^*,\ u_z^*,\ u_r^*,\ u_\phi^*,\ p^*,\ \bar{u}_z^*,\ \bar{u}_\phi^*,\ \bar{p}^*\} = \boldsymbol{f}(\boldsymbol{y};\varepsilon) \tag{3.2}$$

which leave the equations (2.4), (2.5), and (2.6) unchanged when written in the new variables $\boldsymbol{y}^*$:

$$\mathscr{C} = \mathscr{C}^*, \tag{3.3a}$$

$$\mathscr{N}_i = \mathscr{N}_i^*, \tag{3.3b}$$

$$(\mathscr{N}_i u_j + \mathscr{N}_j u_i) = (\mathscr{N}_i u_j + \mathscr{N}_j u_i)^*. \tag{3.3c}$$

The superscript * of any quantity denotes its evaluation according to the transformation (3.2). The purpose of the symmetry analysis is to find the most general form of $\boldsymbol{f}$ in (3.2) which solves the symmetry condition (3.3). A transformation $\boldsymbol{f}$ which solves (3.3) is called a symmetry. If $\boldsymbol{f}$ is implemented into the right-hand side of (3.3) it results in a large nonlinear overdetermined system of partial differential equations for

the mapping function $\boldsymbol{f}$. To find a general solution of this system would be extremely difficult and may also not be desirable. The most general form of the transformation $\boldsymbol{f}$ may be separated into two different sets: finite groups and continuous groups of transformation. The Navier–Stokes equations for example admit finite groups of transformations which are reflection symmetries of the form $\boldsymbol{u}^* = -\boldsymbol{u}$, $\boldsymbol{x}^* = -\boldsymbol{x}$. However, to find self-similar or invariant solutions only the continuous groups of transformations are useful which contain one or several continuous parameters as indicated by ε in (3.2). The frame-invariance transformation $\boldsymbol{x}^* = \boldsymbol{x} + \boldsymbol{a}$ is an example of a continuous transformation group of the Navier–Stokes equations.

The key to find the continuous transformations without any need to investigate the intractably large nonlinear overdetermined system of partial differential equations for $\boldsymbol{f}$ is an infinitesimal form of the transformation (3.2)

$$\boldsymbol{y}^* = \boldsymbol{y} + \varepsilon \left.\frac{\partial \boldsymbol{f}}{\partial \varepsilon}\right|_{\varepsilon=0} + O(\varepsilon^2) \tag{3.4}$$

first introduced by Lie.

It can be shown (see e.g. Bluman & Kumei 1989) that from the expansion (3.4) only terms up to the order e need to be considered, i.e.

$$\left.\begin{gathered} z^* = z + \varepsilon\xi_z,\ \ r^* = r + \varepsilon\xi_r,\ \ \phi^* = \phi + \varepsilon\xi_\phi,\ \ t^* = t + \varepsilon\xi_t,\ \ v^* = v + \varepsilon\xi_v, \\ u_z^* = u_z + \varepsilon\eta_{u_z},\ \ u_r^* = u_r + \varepsilon\eta_{u_r},\ \ u_\phi^* = u_\phi + \varepsilon\eta_{u_\phi},\ \ p^* = p + \varepsilon\eta_p, \\ \bar{u}_z^* = \bar{u}_z + \varepsilon\eta_{\bar{u}_z},\ \ \bar{u}_\phi^* = \bar{u}_\phi + \varepsilon\eta_{\bar{u}_\phi},\ \ \bar{p}^* = \bar{p} + \varepsilon\eta_{\bar{p}}, \end{gathered}\right\} \tag{3.5}$$

where, instead of the mapping $\boldsymbol{f}$, only the infinitesimal generators $\boldsymbol{\xi} = \boldsymbol{\xi}(\boldsymbol{y})$ and $\boldsymbol{\eta} = \boldsymbol{\eta}(\boldsymbol{y})$ need to be determined. The subscripts of the elements of $\boldsymbol{\xi}$ and $\boldsymbol{\eta}$ indicate the variables they refer to and should not to be mistaken as derivatives. Given the infinitesimal generators $\boldsymbol{\xi}$ and $\boldsymbol{\eta}$, the global transformation $\boldsymbol{f}$ is uniquely determined by Lie's differential equations (see e.g. Ibragimov 1994, 1995). The major advantage of the infinitesimal approach is that the equations for the infinitesimal generators are linear and, generally, easy to solve.

To find the infinitesimals $\boldsymbol{\xi}$ and $\boldsymbol{\eta}$, the infinitesimal form of transformation (3.5) will be introduced into the equations (3.3). As an example consider the symmetry condition for the continuity equation $\mathscr{C} = \mathscr{C}^*$ which changes to $\mathscr{C} = \mathscr{C} + \varepsilon \mathrm{X}\mathscr{C} + O(\varepsilon^2)$. The term $\mathscr{C}$ cancels on both sides. As has been mentioned above only the order-ε terms need to be considered and hence the leading-order equation is given by $\mathrm{X}\mathscr{C} = 0$ where X is defined by (3.6) below.

This can be generalized and the symmetries of the equations (2.4) and (2.5) can be calculated by applying the following operator:

$$\begin{aligned} \mathrm{X} = {} & \xi_z \frac{\partial}{\partial z} + \xi_r \frac{\partial}{\partial r} + \xi_\phi \frac{\partial}{\partial \phi} + \xi_t \frac{\partial}{\partial t} + \xi_v \frac{\partial}{\partial v} \\ & + \eta_{u_z} \frac{\partial}{\partial u_z} + \eta_{u_r} \frac{\partial}{\partial u_r} + \eta_{u_\phi} \frac{\partial}{\partial u_\phi} + \eta_p \frac{\partial}{\partial p} + \eta_{\bar{u}_z} \frac{\partial}{\partial \bar{u}_z} + \eta_{\bar{u}_\phi} \frac{\partial}{\partial \bar{u}_\phi} + \eta_{\bar{p}} \frac{\partial}{\partial \bar{p}} \end{aligned} \tag{3.6}$$

and its prolongation (see e.g. Ibragimov 1994, 1995) to the equations (2.4) and (2.5) which yields

$$\mathrm{X}\mathscr{C} = 0 \ \text{ and } \ \mathrm{X}\mathscr{N}_i = 0 \tag{3.7}$$

under consideration of (2.3).

As a result, a set of more than one hundred linear overdetermined partial differential equations for $\boldsymbol{\xi}$ and $\boldsymbol{\eta}$ (not shown here) are obtained. Its solution defines the infinitesimal generators $\boldsymbol{\xi}$ and $\boldsymbol{\eta}$ given in equation (A 1) of the Appendix.

There are still unknown functions in the infinitesimal generators. In particular, the appearance of g_1 and g_2 in (A 1) refers to the fact that the mean velocity profiles for $\bar{u}_z$ and $\bar{u}_\phi$ cannot be determined uniquely. In order to do so the symmetries have to be consistent with the equations (2.6). According to the theory in Oberlack (1997), the operator (3.6) and its prolongation plus the already calculated generators (A 1) will be applied to (2.6) which yields

$$\mathrm{X}(\mathscr{N}_i u_j + \mathscr{N}_j u_i) = 0. \tag{3.8}$$

As a result, the reduced set of generators given by equation (A 2) is obtained. The generators have a similar form to those obtained in Oberlack (1997). In particular, the generators of the fluctuation velocities u_z, u_r, and u_ϕ are such that the proof in appendix A in Oberlack (1997) also applies to the present problem. As a result, no higher-order VPEs need to be considered. The invariance of the equations (2.3)–(2.6) is sufficient for the scaling laws to be consistent with all higher-order correlation equations.

Comparing the resulting infinitesimal generators in some detail with those obtained for plane parallel turbulent shear flows, two major differences appear. First, for the plane case, the coordinate x_2, which is normal to the mean flow $\bar{u}_1$, can have an arbitrary origin. As a result, $\bar{u}_1$ is frame invariant in x_2 and this results in an arbitrary additive constant in the infinitesimal generator for ξ_{x_2}. In the axisymmetric case a corresponding constant is missing, since no shift in the r-direction can be introduced. As will be shown below, this fact restricts the form of the possible invariant solutions. An invariant mean velocity that has an exponential form does not exist for the axisymmetric case.

The second major difference arises because system rotation has different effects on both flows. For the plane case, system rotation imposes a time scale on the flow, which is symmetry breaking, and only the linear mean velocity is an invariant solution. For the present case, system rotation about the z-axis is not symmetry breaking. Additional solid-body rotation terms appear in the subsequent scaling laws for the azimuthal mean velocity. However, the fundamental form of the scaling laws is unaltered.

In the following it will be pointed out how the infinitesimals (A 2) are used to obtain self-similar solutions. In principle the infinitesimal generators (A 2) may be used to compute the global transformations (3.2) (see e.g. Ibragimov 1994, 1995) which in turn may be utilized to derive self-similar solutions. This is not necessary since the similarity variables may be obtained from the infinitesimals directly. It is well known that the defining property of self-similar solutions of a differential equation are their representation by a lower number of independent variables. A less well known but synonymous description of self-similar solutions is by their unaffectedness or invariance due to symmetry transformations. The latter definition will be employed to derive self-similar solutions.

Suppose the self-similar solutions to be derived herein are given by

$$\boldsymbol{z} = \boldsymbol{\Theta}(\boldsymbol{x}), \tag{3.9}$$

where $\boldsymbol{z}$ corresponds to the vector of all dependent variables and $\boldsymbol{x}$ to the vector of all independent variables including v. In implicit form (3.9) may be written as

$$\boldsymbol{F}(\boldsymbol{x},\boldsymbol{z}) = \boldsymbol{z} - \boldsymbol{\Theta}(\boldsymbol{x}) = 0. \tag{3.10}$$

Self-similarity may be formulated through two necessary and sufficient conditions:

(i) $\boldsymbol{F} = 0$ is a solutions of the equations (2.3)–(2.6),

(ii) $\boldsymbol{F}$ is invariant with respect to the symmetry groups admitted by the equations (2.3)–(2.6).

In the methodology of Lie group analysis (ii) may be written as

$$\mathrm{X}\boldsymbol{F} = \mathrm{X}\,[\boldsymbol{z} - \boldsymbol{\Theta}(\boldsymbol{x})]|_{z=\boldsymbol{\Theta}(\boldsymbol{x})} = 0. \tag{3.11}$$

X is defined by (3.6) where the infinitesimals are taken from (A 2) in the Appendix. Carrying out the differentiations of operator X, condition (3.11) may be rewritten as

$$\xi_i(\boldsymbol{x}, \boldsymbol{\Theta}(\boldsymbol{x}))\frac{\partial \boldsymbol{\Theta}}{\partial x_i} = \boldsymbol{\eta}(\boldsymbol{x}, \boldsymbol{\Theta}(\boldsymbol{x})). \tag{3.12}$$

Equation (3.12) may be solved employing the method of characteristics which leads to the set of equations

$$\frac{\mathrm{d}z}{\xi_z} = \frac{\mathrm{d}r}{\xi_r} = \frac{\mathrm{d}\phi}{\xi_\phi} = \frac{\mathrm{d}t}{\xi_t} = \frac{\mathrm{d}v}{\xi_v} = \frac{\mathrm{d}u_z}{\eta_{u_z}} = \frac{\mathrm{d}u_r}{\eta_{u_r}} = \frac{\mathrm{d}u_\phi}{\eta_{u_\phi}} = \frac{\mathrm{d}\bar{u}_z}{\eta_{\bar{u}_z}} = \frac{\mathrm{d}\bar{u}_\phi}{\eta_{\bar{u}_\phi}} = \frac{\mathrm{d}p}{\eta_p} = \frac{\mathrm{d}\bar{p}}{\eta_{\bar{p}}}, \tag{3.13}$$

called the invariant surface condition. As in the classical method of characteristics the constants of integration are to be taken as the new variables. From (3.13) it is apparent that the number of integration constants is one less than the original number of variables and hence a similarity reduction will be achieved.

In the literature it has been argued correctly that in principle all the self-similar solutions or scaling laws may depend on viscosity or Reynolds number. In fact, this can also be taken from the infinitesimals in Appendix which all depend v. However, the exact functional dependence on the Reynolds number cannot be determined from the present form of the theory since the group parameters arbitrarily depend on viscosity. A recent proposal for the functional dependence of near-wall scaling laws on Reynolds number has been made in Barenblatt (1993). On the other side, in an innumerable number of experiments it has been observed that mean quantities become independent of Reynolds number as the Reynolds number tends to infinity. Unfortunately, a solid theoretical foundation for this behaviour has not been given yet. In view of the present self-similarity analysis of high-Reynolds-number flows the large-Reynolds-number limit may be translated to the following weak restriction on the group parameters:

$$\lim_{v\to 0} k(v) = \text{finite}, \tag{3.14}$$

where $k(v)$ is a representative of all group parameters in (A 2). The latter limit does not restrict the number or the functional form of the self-similar solutions to be computed later. The only restriction is that the constants appearing in the self-similar solutions are to be independent of viscosity. An explicit functional Reynolds number dependence in the scaling laws will be investigated in the future, since the functional dependence is beyond the scope of the present analysis.

Recall that the present purpose is to investigate scaling laws for the mean flow. Hence, the following results are restricted to the reduced invariant surface condition for $\bar{u}_z$ and $\bar{u}_\phi$ taken from (3.13)

$$\frac{\mathrm{d}r}{a_1 r} = \frac{\mathrm{d}\bar{u}_z}{[a_1 - a_2]\bar{u}_z + b_1}, \quad \frac{\mathrm{d}r}{a_1 r} = \frac{\mathrm{d}\bar{u}_\phi}{[a_1 - a_2]\bar{u}_\phi - a_2 r\Omega}, \tag{3.15}$$

where the infinitesimal generators in (A 2) have implemented. Each of the group parameters a_1, a_2, b_1 corresponds to a certain physical meaning: a_1 and a_2 conform to two scaling or dilatation groups referring to the fact that in classical mechanics space and time can be arbitrarily stretched; b_1 constitutes the classical Galilean group of transformation. The scaling laws emerging from the conditions (3.15) can be readily integrated and three cases are to be distinguished each one referring to a broken symmetry.

3.1. *Algebraic axial and azimuthal mean velocity profile: $a_1 \neq a_2 \neq 0$ and $b_1 \neq 0$*

This is the most general case and no symmetry breaking scale is imposed on the flow. Equation (3.15) can be integrated for the axial and azimuthal mean velocity:

$$\bar{u}_z = -\frac{b_1}{a_1 - a_2} + C_1 r^{1-a_2/a_1} \tag{3.16}$$

and

$$\bar{u}_\phi = C_2 r^{1-a_2/a_1} - \Omega r, \tag{3.17}$$

respectively, where C_1 and C_2 are constants. In § 4, experimental and DNS data are used to verify the equations (3.16) and (3.17).

A sub-case of the present parameter combination is that of an external time scale acting on the flow, resulting in $a_2 = 0$. The scaling laws for the mean flow would result in a cone-like axial profile and solid-body rotation for the azimuthal mean velocity. So far, such conditions have not been found in a real physical problem.

3.2. *Logarithmic axial mean velocity profile: $a_1 = a_2 \neq 0$ and $b_1 \neq 0$*

This combination of parameters applies if an external velocity scale acts on the flow. For this case the infinitesimal generators for the fluctuation velocities in the generators (A 2) are zero and hence u_z, u_r, and u_ϕ are invariants. As in the case of a plane parallel shear flow, this results in a logarithmic mean velocity profile

$$\bar{u}_z = \frac{b_1}{a_1} \ln(r) + C_3. \tag{3.18}$$

It is important to note that this does not correspond to the classical law of the wall, where the singularity of the logarithm is at the wall; here the singularity appears on the pipe axis (see also § 4). Subsequently is will be referred to as 'circular log-law'. It appears that (3.18) applies in some section of the radius for rapidly rotating pipes, in which the wall velocity is the symmetry-breaking velocity scale. The corresponding azimuthal velocity is given by

$$\bar{u}_\phi = -\Omega r + C_4. \tag{3.19}$$

Of course, (3.19) cannot be valid at the centreline $r = 0$ because of its singular form and it follows that $C_4 = 0$. In general both C_3 and C_4 are constants.

3.3. *Hyperbolic mean velocity profiles: $a_2 = 2a_1 \neq 0$ and $b_1 \neq 0$*

For this parameter combination the infinitesimal generator for ν in (A 2) is zero and hence viscosity is an invariant. The axial mean velocity can be computed to be

$$\bar{u}_z = \frac{b_1}{a_1} + \frac{C_5}{r} \tag{3.20}$$

and the corresponding azimuthal velocity is the potential vortex is given by

$$\bar{u}_\phi = \frac{C_6}{r} - \Omega r. \tag{3.21}$$

This is the only case that is also an invariant solution for a laminar flow because in laminar flows viscosity is always an invariant.

For the subsequent comparison with experimental and DNS data, the system rotation does not need to be considered. In the case of a pipe flow it is fully equivalent if the pipe is put in a rotating coordinate system with a non-moving wall or if the pipe walls are moving in a inertial frame. Owing to the frame rotation, only solid-body rotation terms appear in the scaling laws for the azimuthal velocity. However, it does not alter the form of the scaling law in the inertial frame as has been pointed out above. Without loss of generality, the subsequent investigation is restricted to an inertial frame with $\Omega = 0$.

4. Pipe flow scaling laws in experimental and numerical data

It is important to note that the invariant solutions (3.16)–(3.21) admitted by the equations (2.3)–(2.6) are self-similar solutions. They are not solutions of a boundary value problem for the quantities $\bar{u}_z$ and $\bar{u}_\phi$. Hence, it is not known whether any of the solutions refer to real turbulent flows or whether they can be observed in experimental or DNS data. There is no rigorous proof that turbulence tends towards self-similar solutions when initial and boundary conditions permit this, even though this has been observed in innumerable experimental and DNS data sets. However, Lie group analysis gives strong hints as to which flows the solutions are applicable. This will be explained in the present section and experimental and DNS data will be presented to give an empirical verification of the scaling laws.

The hyperbolic mean velocity profile will not be investigated here, since it is known that straight turbulent vortices in unbounded domains tend to the potential vortex and relaminarize. Donaldson & Bilanin (1975) gave an experimental verification of this, by investigating high-Reynolds-number trailing-edge aircraft vortices. For all the invariant solutions computed here, this is the only case where the mean velocity is an invariant solution for both laminar and turbulent flows. So far, only the axial mean velocity profile (3.20) could not be assigned to any specific turbulent flow.

4.1. *Non-rotating pipe flow*

From the invariant solution (3.16), the proposed new defect law for the pipe flow is given by

$$\frac{\bar{u}_c - \bar{u}_z}{u_\tau} = \chi \left(\frac{r}{R}\right)^{\psi}, \tag{4.1}$$

where χ and ψ are constants. In contrast to the usual defect law for the pipe flow, the coordinate r has its origin at the pipe centre rather than at the pipe wall.

It is important that the functional form of (4.1) is compared with experimental pipe flow data in log-log scaling since linear plots would mask the differences. In figure 1 the data of Zagarola (1996) for high-Reynolds-number turbulent pipe flows are plotted in the form suggested by equation (4.1). (Note that the individual curves are shifted vertically.) The data range about three decades in Reynolds number $Re_m = \bar{u}_m D/\nu$, where the bulk velocity $\bar{u}_m$ is defined by $\bar{u}_m = 2\int_0^R \bar{u}(r) r \mathrm{d}r/R^2$ and D is the pipe diameter.

It is apparent from figure 1 that in the range $0.1 \leqslant r/R \leqslant 0.8$ all data vary linearly. The deviation for $r/R \leqslant 0.1$ may be due to the large amplification of errors when plotting the difference between $\bar{u}_c$ and $\bar{u}_z$ in log coordinates. The data of Zagarola (1996) suggest that the constants in (4.1) are $\chi = 7.5$ and $\psi = 1.77$.

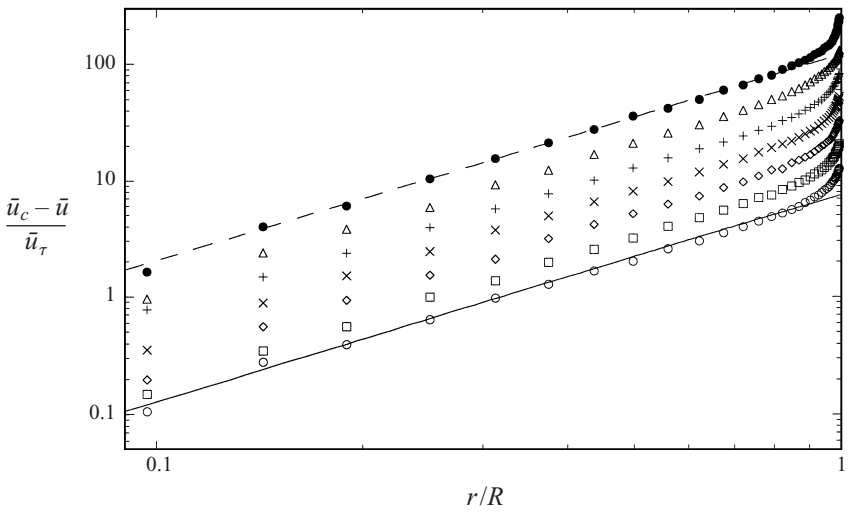

FIGURE 1. Log-log plot of the axial mean velocity of high-Reynolds-number turbulent pipe flow from Zagarola (1996) in defect law scaling (4.1): ○, $Re_m = 3.5 \times 10^7$; □, $Re_m = 1.4 \times 10^7$; ◇, $Re_m = 4.4 \times 10^6$; ×, $Re_m = 1.3 \times 10^6$; +, $Re_m = 4.1 \times 10^5$; △, $Re_m = 1.5 \times 10^5$; •, $Re_m = 4.2 \times 10^4$; ———, $7.5\,(r/R)^{1.77}$; – – –, $10^{1.2}7.5\,(r/R)^{1.77}$. (Beginning with $Re_m = 1.4 \times 10^7$ each data set is shifted upward by the factor $10^{0.2}$.)

The invariant solution (3.16) may have Reynolds number dependence in the exponent and in the coefficient; however this has been explicitly excluded by condition (3.14). Zagarola's data suggest that at least for the medium to high Reynolds numbers presented no such dependence exists. The low-Reynolds-number dependence is beyond the scope of the theory in its present form.

4.2. *Rotating pipe flow*

In contrast to the laminar flow in a rotating pipe, where the azimuthal velocity closely follows solid-body rotation (Reich 1988), in the turbulent flow case, an algebraic scaling law (3.17) is apparent in many experimental and DNS data. This can be rewritten as

$$\frac{\bar{u}_\phi}{\bar{u}_w} = \zeta \left(\frac{r}{R}\right)^{\hat{\psi}}, \tag{4.2}$$

where $\bar{u}_w$ is the azimuthal velocity at the wall and ζ and $\hat{\psi}$ are constants.

In figure 2 experimental data for the azimuthal mean velocity in rotating pipes at moderate rotation numbers are presented. This indicates that for the outer part of the pipe radius the data closely follow an algebraic scaling law, and the range of validity depends on Reynolds number and rotation number $N = \bar{u}_w/\bar{u}_m$. The inner region of the rotating pipe exhibits a deviation from the power law. This is due to measurement errors and in particular to the effect of solid-body rotation that appears near the pipe axis. This will be confirmed below using the DNS data of Orlandi & Fatica (1997) in figure 4.

The data available in the literature indicate that the algebraic scaling law and its exponent have neither a significant Reynolds number nor a rotation number dependence. Only the extension towards the pipe axis is affected by these two parameters. Experiments suggest $\hat{\psi} \approx 2$ and $\zeta \approx 1$.

One can deduce from the two invariant solutions (3.16) and (3.17) that the exponent

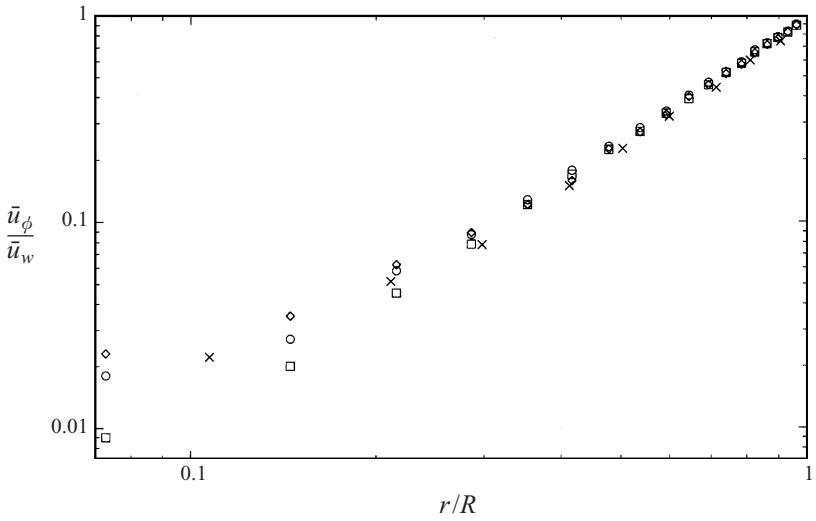

FIGURE 2. Log-log plot of the azimuthal mean velocity normalized with the wall velocity for rotating pipes: ○, $Re_m = 20\,000$, $N = 0.5$; □, $Re_m = 20\,000$, $N = 1.0$; ◇, $Re_m = 50\,000$, $N = 0.5$ (Reich 1988): ×, $Re_m = 50\,000$, $N = 1.0$ (Kikuyama *et al.* 1983).

ψ of the scaling law for the axial velocity in (4.1) is also a constant that has the same value as $\hat{\psi}$. The scaling law in equation (4.1) has to be extended to account for rotation effects in the pre-factor χ, the reason being the following.

There is a fundamental difference in rotating a laminar and a turbulent pipe flow along its axis. In a laminar pipe flow the two-dimensional material frame indifference theorem applies (see e.g. Batchelor 1967). It reflects the fact that a flow is not affected by constant system rotation if the dependent variables only depend on two spatial coordinates and the rotation vector is aligned with the axis of independence. A three-dimensional correspondence for the material indifference theorem does not exist because the Coriolis terms cannot be absorbed within any of the other terms in the Navier–Stokes equations. Since a turbulent flow is always three-dimensional system rotation strongly affects turbulence with growing effectiveness if rotation rate increases. Hence, rotation rate, or for the pipe flow the wall velocity, is an important flow parameter. This leads to the reverse of the material indifference theorem which holds in a weaker form: with increasing rotation rate a turbulent flow becomes more and more two-dimensional and ultimately fully two-dimensional at infinite rotation rate. This is also known as the Taylor–Proudman theorem.

Applied to the rotating pipe problem the scaling law is strongly affected by the additional velocity scale $\bar{u}_w$. Hence, a modified scaling law for axial mean velocity is proposed:

$$\frac{\bar{u}_c - \bar{u}_z}{u_\tau} = \hat{\chi}\left(\frac{\bar{u}_w}{u_\tau}\right)\left(\frac{r}{R}\right)^{\hat{\psi}}, \tag{4.3}$$

where $\hat{\chi}$ is not a constant but rather a function of the velocity ratio.

In figure 3 experimental data of the axial and azimuthal mean velocity have been plotted in log-log scaling for a moderate rotation number. The two curves are parallel and straight for some part of the pipe radius as suggested by (4.2) and (4.3). No functional form has been assigned to $\hat{\chi}\left(\bar{u}_w/u_\tau\right)$ from the present form of the Lie group theory and there is also only a limited amount of data available in the literature.

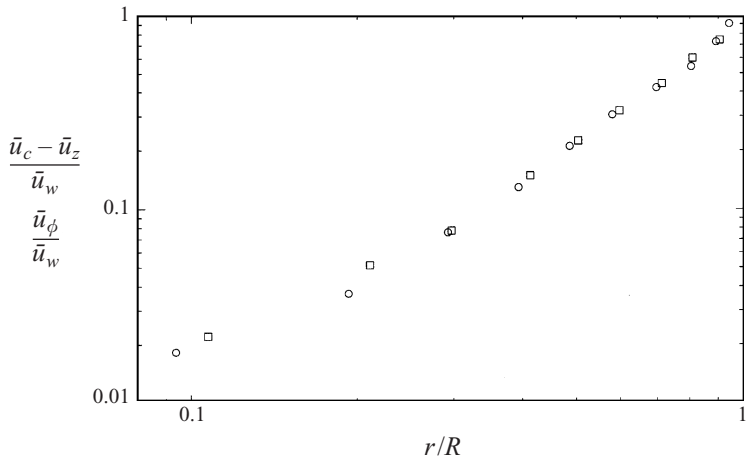

FIGURE 3. Log-log plot of the axial and azimuthal mean velocity of the experimental data of Kikuyama *et al.* (1983) for $Re_m = 50\,000$ and $N = 1.0$ for rotating pipes: ○, $(\bar{u}_c - \bar{u}_z)/\bar{u}_w$: □, $\bar{u}_\phi/\bar{u}_w$.

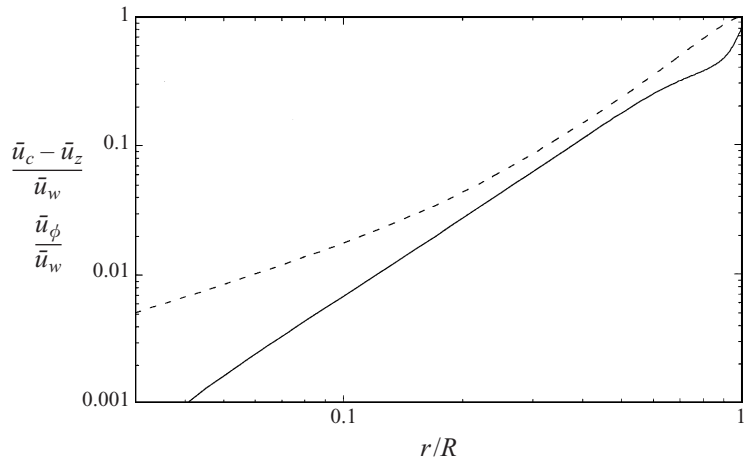

FIGURE 4. Log-log plot of the axial and azimuthal mean velocity of the DNS data of Orlandi & Fatica (1997) for $Re_m = 4900$ and $N = 2$: ——, $(\bar{u}_c - \bar{u}_z)/\bar{u}_w$: – – –, $\bar{u}_\phi/\bar{u}_w$.

Note that (4.2) and (4.3) only apply for moderate rotation number N. As the rotation number increases, the rotating wall velocity $\bar{u}_w$ becomes the dominant velocity scale and the axial velocity changes drastically. In figure 4 the DNS results of Orlandi & Fatica (1997) are plotted for $N = 2$ in log-log scaling. The algebraic law for the axial velocity is reduced significantly and it is only valid up to $r/R \approx 0.5$. The algebraic law for the azimuthal velocity is valid for $0.3 \leqslant r/R \leqslant 0.6$. Below $r/R \approx 0.1$ solid-body rotation is present as mentioned above.

It has already been pointed out that the circular log-law given by (3.18) does not correspond to the usual law of the wall found by von Kármán (1930). The logarithmic singularity is not on the pipe wall but rather on the pipe axis. For the derivation of (3.18) it was assumed that the region of applicability is dominated by an external velocity scale. It appears that the new log-region is valid when $\bar{u}_w$ dominates the

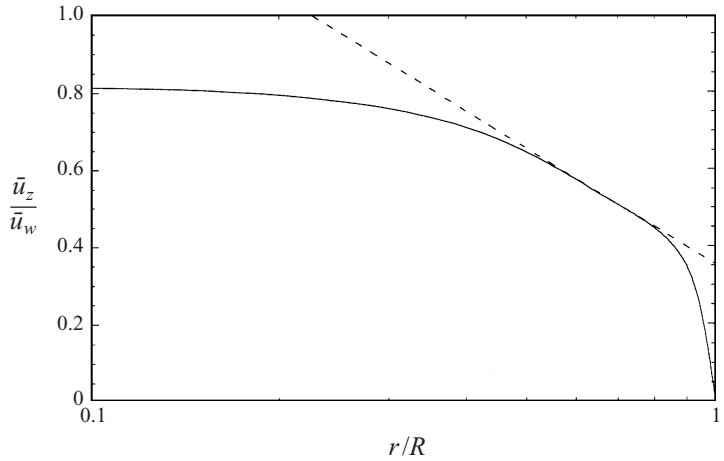

FIGURE 5. Semi-log plot of the axial mean velocity of the DNS data of Orlandi & Fatica (1997) for $Re_m = 4900$ and $N = 2$: ——, $\bar{u}_z/\bar{u}_w$ from DNS: - - - -, $\bar{u}_z/\bar{u}_w = -\log\left(r/R\right) + 0.354$.

friction velocity u_τ. The suggested scaling law is

$$\frac{\bar{u}_z}{\bar{u}_w} = \lambda \log\left(\frac{r}{R}\right) + \omega. \tag{4.4}$$

In figure 5 the axial mean velocity data of Orlandi & Fatica (1997) are now plotted in semi-log scaling, corresponding to (4.4). A straight line matches about 30% of the pipe radius in the range $0.5 \leqslant r/R \leqslant 0.8$. The region of applicability of this new log region is different from the logarithmic law of the wall which lies in the range $0.9 \leqslant r/R \leqslant 1.0$. Also the coefficient λ in (4.4) is negative and approximately equal to -1. The additive constant ω has been fitted to 0.354. Figure 5 plotted in linear scaling (not shown here) exhibits two inflection points which correspond to the 'edges' of the logarithmic scaling law.

5. Near-wall scaling laws

Though a new logarithmic law was found in the previous sections, the group analysis in §3 does not reveal the usual log region near the pipe wall. This is somewhat surprising since it is one of the solutions found by Oberlack (1997) for the case of plane parallel turbulent shear flows. Experimental data of Zagarola & Smits, (1997) suggest that the log region may be valid in the region $0.9 \leqslant r/R \leqslant 1.0$. This near-wall region on the pipe radius is where the pipe curvature has the weakest influence on the flow and hence a regular expansion for large pipe radius may be applicable. Subsequently it will be shown that the leading-order terms in the near-wall region are equivalent to the equations for the flat plate.

In order to do this, a new coordinate system

$$z = z, \;\; y = R - r, \;\; s = r\phi, \;\; U_z = U_z, \;\; U_y = -U_r, \;\; U_s = U_\phi \tag{5.1}$$

according to the sketch in figure 6 is introduced into the equations (2.1) and (2.2). The coordinate s varies along the arc and the coordinate y is a wall-based coordinate pointing towards the centre of the pipe. R is the pipe radius. To identify the leading-order terms in the near-wall region the new coordinates (5.1) will be

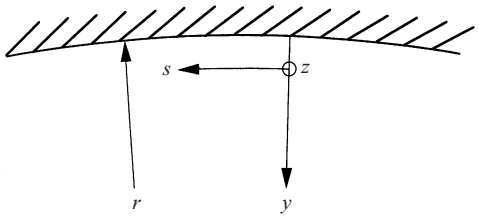

FIGURE 6. Sketch of the wall-based coordinate system as adopted for the near-wall scaling laws.

non-dimensionalized by

$$u_\tau = \left(\nu \left. \frac{\partial \bar{u}}{\partial y} \right|_{y=0} \right)^{1/2} \quad \text{and} \quad l^+ = \nu / u_\tau, \tag{5.2}$$

the friction velocity and the viscous length scale, respectively. Implementing (5.1) and (5.2) into (2.1) and (2.2) yields

$$\frac{\partial U_z}{\partial t} + U_z \frac{\partial U_z}{\partial z} + U_y \frac{\partial U_z}{\partial y} + U_s \frac{\partial U_z}{\partial s} + \frac{s}{y - Re_R} U_y \frac{\partial U_z}{\partial s} = -\frac{\partial P}{\partial z} + \frac{\partial^2 U_z}{\partial z^2} + \frac{\partial^2 U_z}{\partial y^2} + \frac{\partial^2 U_z}{\partial s^2} + \frac{2 s^{1/2}}{y - Re_R} \frac{\partial}{\partial s} \left(s^{1/2} \frac{\partial U_z}{\partial y} \right) + \frac{s}{(y - Re_R)^2} \frac{\partial}{\partial s} \left(s \frac{\partial U_z}{\partial s} \right), \tag{5.3a}$$

$$\frac{\partial U_y}{\partial t} + U_z \frac{\partial U_y}{\partial z} + U_y \frac{\partial U_y}{\partial y} + U_s \frac{\partial U_y}{\partial s} + \frac{1}{y - Re_R} \left(\frac{s}{2} \frac{\partial U_y^2}{\partial s} - U_s^2 \right) = -\frac{\partial P}{\partial y} - \frac{s}{y - Re_R} \frac{\partial P}{\partial s} + \frac{\partial^2 U_y}{\partial z^2} + \frac{\partial^2 U_y}{\partial y^2} + \frac{\partial^2 U_y}{\partial s^2} + \frac{1}{y - Re_R} \left[2 s^{1/2} \frac{\partial}{\partial s} \left(s^{1/2} \frac{\partial U_y}{\partial y} \right) - 2 \frac{\partial U_s}{\partial s} \right] + \frac{1}{(y - Re_R)^2} \left(s^2 \frac{\partial^2 U_y}{\partial s^2} + 2 s \frac{\partial U_y}{\partial s} - U_y \right), \tag{5.3b}$$

$$\frac{\partial U_s}{\partial t} + U_z \frac{\partial U_s}{\partial z} + U_y \frac{\partial U_s}{\partial y} + U_s \frac{\partial U_s}{\partial s} + \frac{1}{y - Re_R} \left(s \frac{\partial U_s}{\partial s} + U_s U_y \right) = -\frac{\partial P}{\partial s} + \frac{\partial^2 U_s}{\partial z^2} + \frac{\partial^2 U_s}{\partial y^2} + \frac{\partial^2 U_s}{\partial s^2} + \frac{1}{y - Re_R} \left[2 s^{1/2} \frac{\partial}{\partial s} \left(s^{1/2} \frac{\partial U_s}{\partial y} \right) + 2 \frac{\partial U_y}{\partial s} \right] + \frac{1}{(y - Re_R)^2} \left(s^2 \frac{\partial^2 U_s}{\partial s^2} + 2 s \frac{\partial U_s}{\partial s} - U_s \right), \tag{5.3c}$$

and

$$\frac{\partial U_z}{\partial z} + \frac{\partial U_y}{\partial y} + \frac{\partial U_s}{\partial s} + \frac{1}{y - Re_R} \frac{\partial}{\partial s} (s U_y) = 0 \tag{5.4}$$

where any indices referring to the non-dimensional form of the equations have been

omitted. In (5.3) and (5.4) the Reynolds number is defined as

$$Re_R = \frac{u_\tau R}{\nu}, \tag{5.5}$$

which can also be interpreted as a normalized pipe radius.

In the limit of an asymptotically large difference between the Reynolds number Re_R and the wall distance y, the leading-order terms of the equations (5.3) and (5.4) are the Navier–Stokes equations in Cartesian coordinates. This is exactly the form of the equations that has been investigated by Oberlack (1997). Compared with the nomenclature therein the present independent variables z, y and s, respectively, refer to the mean flow direction, the wall normal direction and the spanwise direction with the corresponding velocities U_z, U_y and U_s.

Transferring his results to the present problem of the near-wall scaling laws in turbulent pipe flows by adopting the leading-order equations in (5.3) and (5.4), the mean flow profiles can be obtained from the invariant surface condition

$$\frac{\mathrm{d}y}{c_1 y + c_3} = \frac{\mathrm{d}\bar{u}_z}{[c_1 - c_4]\bar{u}_z + d_1}. \tag{5.6}$$

Depending on the choice of the group parameter c_1, c_3, c_4 and d_1, these equations admits five distinct solutions which are a logarithmic, an algebraic, an exponential and two, from a symmetry point of view, different linear mean velocity profiles. A detailed discussion on the different solutions and an empirical verification investigating DNS and experimental data has been given in Oberlack (1997).

The results presented therein also shed some light on a recent controversial discussion in the literature on whether the so-called log region indeed matches a logarithmic function or may instead follow an algebraic scaling law. Proposals towards this idea have been made by Barenblatt (1993), Barenblatt & Chorin (1996), George (1996) and George, Castillo & Knecht (1996).

From the difference $y - Re_R$ in the equations (5.3) and (5.4) it is apparent that with increasing Reynolds number the validity region of the leading-order equations expands. Zagarola & Smits, (1997) have shown that the logarithmic region extends up to about $y = 0.1R$. Using this as an upper bound for y in the equations (5.3) and (5.4) the difference $y - Re_R$ only scales with Re_R. Written in wall coordinates, the length of the log-region increases with Reynolds number, which is well known from experiments in turbulent pipe flows. An example illustrating this has been depicted in figure 7 in which the Reynolds number Re_R varies between 1.1×10^3 and 5.3×10^5.

6. Fixed point analysis

As mentioned in the introduction, Preston (1950) first found a fixed point in the mean velocity profile of a turbulent pipe flow when the mean velocity is normalized with the bulk velocity. In figure 8 the plot by Zagarola *et al.* (1996) is reproduced, showing that the fixed point defines the location where the normalized mean velocity becomes independent of the Reynolds number.

The following analysis is based on the algebraic mean velocity profile defined in equation (4.1). Recall that the algebraic scaling law is valid only for about 80% of the pipe diameter (figure 1) and does not match the no-slip boundary condition. However, the present analysis captures the basic features of the fixed point and gives estimates for its location. Also, a simple explanation for a new outer scaling law introduced by Zagarola (1996) can be provided.

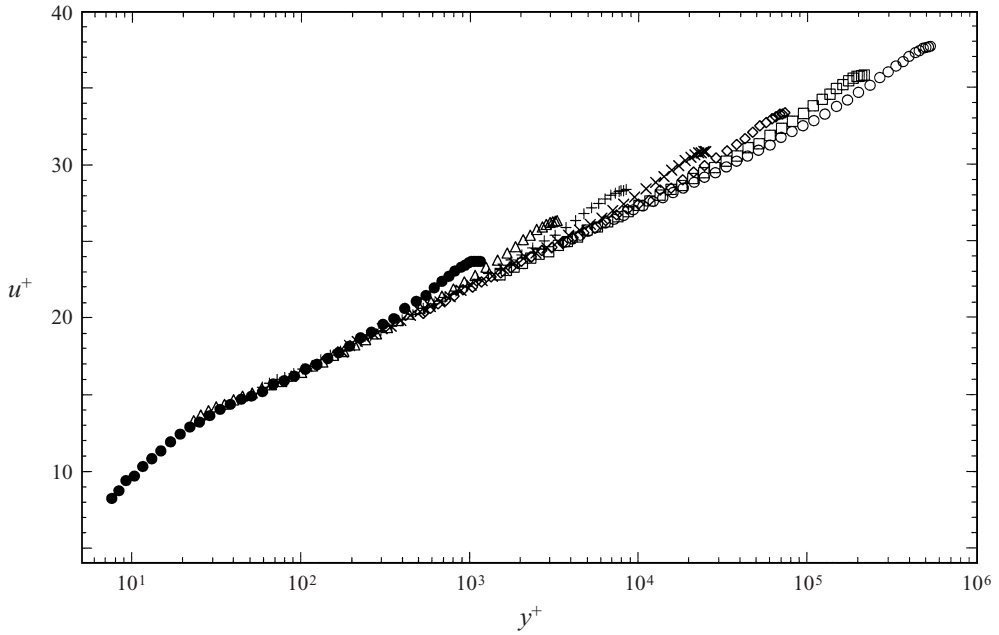

FIGURE 7. Semi-logarithmic plot of the axial mean velocity of high-Reynolds-number turbulent pipe flow from Zagarola (1996) in near-wall scaling. The data cover the range from the viscous sub-layer to the pipe axis: ○, $Re_m = 3.5 \times 10^7$; □, $Re_m = 1.4 \times 10^7$; ◇, $Re_m = 4.4 \times 10^6$; ×, $Re_m = 1.3 \times 10^6$; +, $Re_m = 4.1 \times 10^5$; △, $Re_m = 1.5 \times 10^5$; ●, $Re_m = 4.2 \times 10^4$.

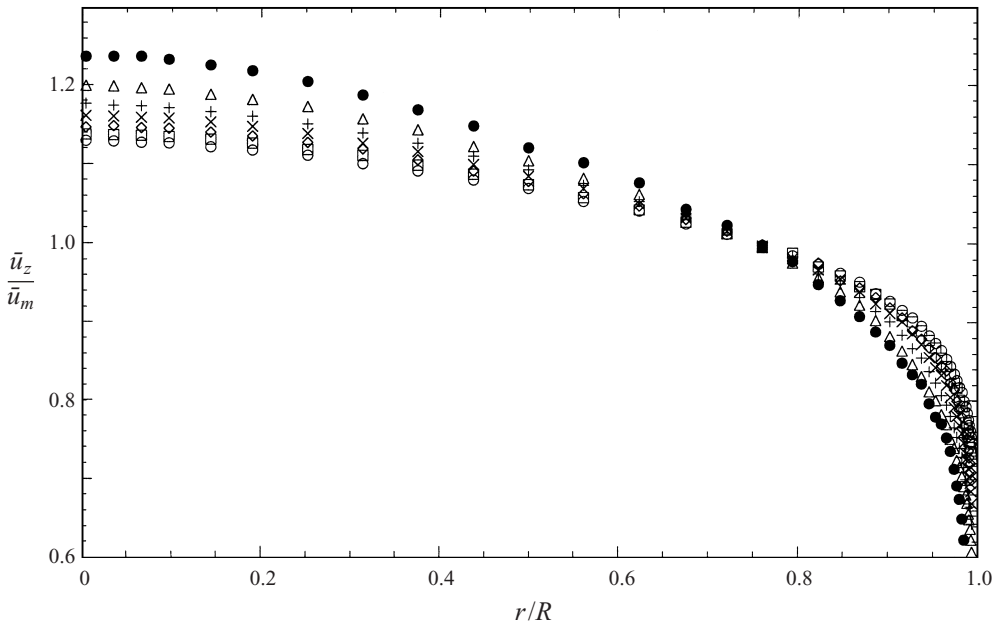

FIGURE 8. Mean velocity normalized with the bulk velocity in high-Reynolds-number turbulent pipe flow from Zagarola (1996) ○, $Re_m = 3.5 \times 10^7$; □, $Re_m = 1.4 \times 10^7$; ◇, $Re_m = 4.4 \times 10^6$; ×, $Re_m = 1.3 \times 10^6$; +, $Re_m = 4.1 \times 10^5$; △, $Re_m = 1.5 \times 10^5$; ●, $Re_m = 4.2 \times 10^4$.

It is interesting to note that the fixed-point analysis to follow also holds for the rotating pipe flow. It can be seen from the scaling law (4.3) that the rotation rate or the wall velocity only appears in the coefficient of the algebraic function. Subsequently it will be shown that to leading order the fixed point is only determined by the exponent of the algebraic scaling law. Hence, the ensuing calculation also provides a basis for the fixed point observed in rotating pipe flow when the rotation number is varied. Examples for this phenomena at several different but large Reynolds numbers have been reported by Reich (1988).

Assuming equation (4.1) to be valid for the entire pipe diameter, the mean bulk velocity can be calculated as

$$\bar{u}_m = \bar{u}_c - \frac{2\chi}{2+\psi} u_\tau. \tag{6.1}$$

Rewriting the latter equation, one obtains that u_τ is proportional to $\bar{u}_c - \bar{u}_m$, as has already been proposed by Zagarola (1996) as part of a modified defect scaling law for the turbulent pipe flows. Considering (6.1) in the form $u_\tau/(\bar{u}_c - \bar{u}_m) = (2+\psi)/(2\chi)$, the left- and the right-hand sides may be evaluated separately from the measured data and the theory. Employing the coefficients of equation (4.1) taken from Zagarola's data, a factor of $(2+\psi)/(2\chi) = 0.251$ is obtained. Using the values for the three velocity scales u_τ, $\bar{u}_c$ and $\bar{u}_m$ taken directly from the experiment, a slightly smaller value of $u_\tau/(\bar{u}_c - \bar{u}_m) = 0.232$ is obtained.

Equation (6.1) may be combined with (4.1) to get the form

$$\frac{\bar{u}}{\bar{u}_m} = \frac{1 - \chi\left(\dfrac{r}{R}\right)^\psi \dfrac{u_\tau}{\bar{u}_c}}{1 - \dfrac{2\chi}{2+\psi}\dfrac{u_\tau}{\bar{u}_c}}. \tag{6.2}$$

Since the fixed point is independent of the Reynolds number, the derivative of equation (6.2) with respect to Re is taken and the resulting expression is set to zero. In (6.2) only $u_\tau/\bar{u}_c$ depends on the Reynolds number. After some algebra an estimate for the fixed point location is obtained

$$r_{fix} = R\left(\frac{2}{2+\psi}\right)^{1/\psi}, \tag{6.3}$$

which only depends on the exponent and not on the pre-factor of the power law (4.1). Employing the exponent $\psi = 1.77$, matched to Zagarola's data, in the fixed-point approximation (6.3) yields $r_{fix} = 0.7R$ which is within 10% of the measured value of $r_{fix} = 0.75R$. Substituting (6.3) into the equation for the mean velocity (6.2), $\bar{u}/\bar{u}_m = 1$ is obtained, as observed in experimental data.

To assess the validity of using the algebraic mean velocity over the entire pipe diameter, the deviations for three quantities given by theory and the measured values in Zagarola (1996) are compared. The difference between the bulk velocity from (6.1) and Zagarola's data is less than 3%. The factor $(2+\psi)/(2\chi)$ is within 8% of the experiments and the error for the fixed point is about 10%.

As mentioned above the fixed point analysis also holds for the flow in a rotating pipe when the rotation rate is varied. Reich's data exhibit a slightly smaller value for the fixed point at $r_{fix} \approx 0.7R$ which is closer to the calculated value in the present analysis.

7. Discussion and conclusions

It has been demonstrated that the approach developed in Oberlack (1997), based on Lie group theory, can be used to derive several new scaling laws for high-Reynolds-number turbulent flows in a non-rotating and rotating pipe. The key issue in the present work is that the scaling laws have been derived from the Navier–Stokes equations using Lie group methods. The analysis includes two algebraic laws for the axial and the azimuthal mean velocity and a logarithmic law for the axial mean velocity. All the scaling laws, which are also called self-similar or invariant solutions, scale on the distance from the centreline rather than with the wall distance, in contrast to the classical wall-based scaling laws.

In a non-rotating pipe, the algebraic law for the axial velocity covers about 80% of the pipe radius. This was confirmed for three decades of Reynolds number by using the data of Zagarola (1996). In the case of the rotating pipe flow the algebraic law for the azimuthal velocity was confirmed for a range of Reynolds numbers and rotation numbers for at least 70% of the radius. Based on experimental and DNS data it was concluded that, except in the central region of the pipe, these scaling laws were independent of Re and Ω.

For high rotation numbers, the azimuthal velocity at the wall (rather than the friction velocity) becomes the dominant velocity scale imposed on the flow, and in this case a new logarithmic law is found. The validity of this law was demonstrated by using the DNS data of Orlandi & Fatica (1997) at the rotation number $N = 2$. The new circular log law differs from the usual log law of the wall because it scales with the radius and its location is closer to the pipe axis and has a wider extent.

Based on the equations of motion in cylindrical coordinates the classical near-wall scaling laws have not been captured. An asymptotic expansion of the Navier–Stokes equations on the curved wall has been employed to show that near-wall scaling laws can be obtained from flat-surface scaling laws in the limit of large Reynolds numbers. As a result, all the near-wall scaling laws obtained in Oberlack (1997) also apply to the present approach.

The point on the pipe radius where all mean velocities collapse when normalized with bulk velocity is known as the fixed point, and its position is independent of Reynolds number and rotation number. By using the algebraic law for the axial mean velocity an estimate for the position of the fixed point is given for both the non-rotating and the rotating pipe.

Even though the present theory gives a sound theoretical basis for turbulent scaling laws derived from first principles some unresolved questions in rotating and non-rotating turbulent pipe flows still remain. All scaling laws only apply in certain regions and no link between different scaling laws has been given. Also the extent of the scaling laws cannot be predicted. In addition, the constants in the scaling laws had to be taken from the experimental or DNS data. All these questions will be the subject of future research and will be addressed in an extension of the present theory.

The author is very much indebted to Peter Bradshaw, Nail H. Ibragimov, Thomas S. Lund, Michael M. Rogers, Seyed G. Saddoughi, and Alan A. Wray for reading the manuscript at several stages of its development and giving valuable comments. Special thanks to Rainer Friedrich with whom the author had inspiring discussions about near-wall scaling laws. Furthermore he thanks Alexander J. Smits, H. Beer, Bendiks J. Boersma and Massimiliano Fatica for the kind cooperation and providing

data. The author also very much appreciated the referees' valuable suggestions. The work was in part supported by the Deutsche Forschungsgemeinschaft under grant number Ob 96/2-1.

Appendix. Infinitesimal generators

The condition (3.7) results in the following set of infinitesimal generators:

$$\xi_z = a_1(v)z + f_1(t,v), \quad \xi_r = a_1(v)r, \quad \xi_\phi = -a_2(v)t\Omega + a_3(v), \tag{A1 a–c}$$

$$\xi_t = a_2(v)t + a_4(v), \quad \xi_v = [2a_1(v) - a_2(v)]v, \tag{A1 d,e}$$

$$\eta_{u_z} = [a_1(v) - a_2(v)](\bar{u}_z + u_z) + \frac{\mathrm{d}f_1}{\mathrm{d}t} - g_1(r,v,\bar{u}_z,\bar{u}_\phi,\bar{p}), \tag{A1 f}$$

$$\eta_{u_r} = [a_1(v) - a_2(v)]u_r, \tag{A1 g}$$

$$\eta_{u_\phi} = [a_1(v) - a_2(v)](\bar{u}_\phi + u_\phi) - g_2(r,v,\bar{u}_z,\bar{u}_\phi,\bar{p}) - a_2(v)r\Omega, \tag{A1 h}$$

$$\eta_p = 2[a_1(v) - a_2(v)](\bar{p} + p) - z\left[\frac{\mathrm{d}^2 f_1}{\mathrm{d}t^2} + [a_1(v) - 2a_2(v)]K\right] - g_3(r,v,\bar{u}_z,\bar{u}_\phi,\bar{p}) - a_2(v)r^2\Omega^2 + f_2(t,v), \tag{A1 i}$$

$$\eta_{\bar{u}_z} = g_1(r,v,\bar{u}_z,\bar{u}_\phi,\bar{p}), \quad \eta_{\bar{u}_\phi} = g_2(r,v,\bar{u}_z,\bar{u}_\phi,\bar{p}), \quad \eta_{\bar{p}} = g_3(r,v,\bar{u}_z,\bar{u}_\phi,\bar{p}) \tag{A1 j–l}$$

where all group parameters depend on v. The additional condition for the velocity product equations (3.8) results in the reduced set of infinitesimal generators

$$\xi_z = a_1(v)z + b_1(v)t + b_2(v), \quad \xi_r = a_1(v)r, \ \xi_\phi = -a_2(v)t\Omega + a_3(v), \tag{A2 a–c}$$

$$\xi_t = a_2(v)t + a_4(v), \quad \xi_v = [2a_1(v) - a_2(v)]v, \tag{A2 d,e}$$

$$\eta_{u_z} = [a_1(v) - a_2(v)]u_z, \quad \eta_{u_r} = [a_1(v) - a_2(v)]u_r, \quad \eta_{u_\phi} = [a_1(v) - a_2(v)]u_\phi, \tag{A2 f–h}$$

$$\eta_p = 2[a_1(v) - a_2(v)]p - h_1(r,v) - z[a_1(v) - 2a_4(v)]K - a_2(v)r^2\Omega^2 + f_3(t,v), \tag{A2 i}$$

$$\eta_{\bar{u}_z} = [a_1(v) - a_2(v)]\bar{u}_z + b_1(v), \quad \eta_{\bar{u}_\phi} = [a_1(v) - a_2(v)]\bar{u}_\phi - a_2(v)r\Omega,$$
$$\eta_{\bar{p}} = 2[a_1(v) - a_2(v)]\bar{p} + h_1(r,v). \tag{A2 j–l}$$

REFERENCES

Barenblatt, G. I. 1993 Scaling laws for fully developed turbulent shear flows. Part 1. Basic hypotheses and analysis. *J. Fluid Mech.* **248**, 513–520.

Barenblatt, G. I. & Chorin, A. J. 1996 Scaling laws and zero viscosity limits for wall-bounded shear flows and for local structure in developed turbulence. *Center for Pure and Applied Mathematics, UC Berkeley, PAM*-678.

Batchelor, G. K. 1967 *An Introduction to Fluid Dynamics*. Cambridge University Press.

Bluman, G. W. & Kumei, S. 1989 *Symmetries and Differential Equations*. Applied Mathematical Sciences, vol. 81. Springer.

Champagne, B., Hereman, W. & Winternitz, P. 1991 The computer calculation of Lie point symmetries of large systems of differential equations. *Comput. Phys. Commun.* **66**, 319–340.

Darcy, P. 1858 Recherches expérimentales relative aux mouvements de l'eau dans tuyaux. *Mem. Prés. l'Acad. Sci. l'Institut de France* **15**, 141.

Donaldson, du P. C. & Bilanin, A. J. 1975 Vortex wakes of conventional aircraft. *AGARD* AG-204.

Eggels, J. G. M., Boersma, B. J. & Nieuwstadt, F. T. M. 1996 Direct and large eddy simulation of turbulent flow in an axially rotating pipe. *Submitted to J. Fluid Mech.*

George, W. K. & Castillo, L. 1996 A theory for turbulent pipe and channel flows. Presented at *Disquisitiones Mechanicae at the University of Illinois.*

George, W. K., Castillo, L. & Knecht, P. 1996 The zero pressure-gradient turbulent boundary layer. *Turbulence Research Laboratory, School of Engineering and Applied Sciences, SUNY Bufallo, NY, Tech. Rep.* TRL-153.

Hill, J. M. 1992 *Differential Equations and Group Methods for Scientists and Engineers.* CRC Press.

Hirai, S., Takagi, T. & Matsumoto, M. 1988 Predictions of the laminarization phenomena in an axially rotating pipe flow. *Trans. ASME: J. Fluids Engng* **110**, 424–430.

Ibragimov, N. H. (ED.) 1994, 1995 *CRC Handbook of Lie Group Analysis of Differential Equations, Vols. 1-3.* CRC Press.

Ibragimov, N. H. & Ünal, G. 1994 Lie groups in turbulence. *Lie Groups and Their Applics.* **1**(2), 98–103.

Jones, W. P. & Launder, B. E. 1973 The calculation of low-Reynolds number phenomena with a two-equation model of turbulence. *Intl J. Heat Mass Transfer* **16**, 1119–1130.

Kármán, Th. von 1930 Mechanische Ähnlichkeit und Turbulenz. *Proc. 3rd Intl Congress for Applied Mechanics, Stockholm 24–29 August 1930*, Vol. 1, pp. 85–93.

Kikuyama, K., Murakami, M., Nishibori, K. & Maeda, K. 1983 Flow in axially rotating pipe. *Bull. JSME* **26**, 506–513.

Launder, B. E., Priddin, C. H. & Sharma, B. I. 1977 The calculation of turbulent boundary layers on spinning and curved surfaces. *Trans. ASME: J. Fluids Engng* **99**, 231–239.

Launder, B. E., Reece, G. H. & Rodi, W. 1975 Progress in the developement of a Reynolds-stress turbulence closure. *J. Fluid Mech.* **68**, 537–566.

Levy, F. 1929 Strömungserscheinungen in rotierenden Rohren. *VDI Forschungs. auf dem Gebiet der Ing.* **322**, 18–45.

MACSYMA 1993 *Mathematics Reference Manual.* Macsyma Inc.

Murakami, M. & Kikuyama, K. 1980 Turbulent flow in axially rotating pipes. *Trans. ASME: J. Fluids Engng* **102**, 97–103.

Oberlack, M. 1997 Unified theory for symmetries in plane parallel turbulent shear flows. *Center for Turbulence Research, NASA Ames/Stanford University, Manuscript* 163 (also submitted to *J. Fluid Mech.*)

Olver, P. J. 1986 *Applications of Lie Groups to Differential Equations.* Graduate Texts in Mathematics, Vol. 107. Springer.

Orlandi, P. & Fatica M. 1997 Direct simulations of turbulent flow in a pipe rotating about its axis. *J. Fluid Mech.* **343**, 43–72.

Prandtl, L. 1925 Über die ausgebildete Turbulenz. *Z. Angew. Math. Mech.* **5**, 136–139.

Preston, J. H. 1950 The three-quarter radius pitot tube flow meter. *The Engineer* **190**, 400–403.

Reich, G. 1988 Strömung und Wärmeübertragung in einem axial rotierenden Rohr. Doctoral Thesis, Darmstadt University.

Schlichting, J. C. 1979 *Boundary-Layer Theory.* McGraw-Hill.

Stanton, T. E. & Pannel, J. R. 1914 Similarity of motion in relation of the surface friction of fluids. *Phil. Trans. R. Soc. Lond.* A **214**, 199.

Ünal, G. 1994 Application of equivalence transformations to inertial subrange of turbulence. *Lie Groups and Their Applics.* **1**(1), 232–240.

Zagarola, M. V. 1996 Mean-flow scaling of turbulent pipe flow. PhD Thesis, Princeton University.

Zagarola, M. V. & Smits, A. J. 1997 Scaling of the mean velocity profile for turbulent pipe flow. *Phys. Rev. Lett.* **78**, 239-242.

Zagarola, M. V., Smits, A. J., Orszag, S. A. & Yakhot V. 1996 Experiments in high Reynolds number turbulent pipe flow *AIAA Paper* 96-0654.